

**GAIN AND PHASE DETECTOR BASED ON
THE ANALOG DEVICES AD8302 CHIP**

David Cuadrado Calle, José Antonio López Pérez

INFORME TÉCNICO - CAY 2012 - 5
Marzo 2012

ÍNDEX

1. Introduction	2
2. Description of the circuit	2
3. Block diagram	3
4. PCB circuit design.....	4
5. Measurements.....	5
6. Conclusions	12
7. Acknowledgments	12
Appendix A: Box enclosure drawings.....	13
Appendix B: Datasheets.....	14

1. Introduction

This report shows the design and implementation of an evaluation board for the *Analog Devices* AD8302 chip. This integrated circuit measures the gain and the phase differences between two RF input signals from DC to 2.7GHz, according to its datasheet (see appendix B).

This circuit could be used in applications where relative amplitude and phase measurements are needed, like microwave holography.

2. Description of the circuit

The AD8302 is a fully integrated system for measuring gain/loss and phase in numerous applications. The PCB circuit described in this report, provides the AD8302 with all the auxiliary components for its proper operation. The PCB is installed into an aluminium box that has been designed to fit with the board dimensions (see appendix A).

The PCB circuit is equipped with two SMA input connectors for the two RF input signals, whose relative gain and phase are to be measured, and two SMA output connectors, named “Vmag” and “Vphs”, for the output signals. In “Vmag” there is a voltage proportional to the gain or loss between the two input channels while in “Vphs” the voltage is proportional to the phase difference.

The gain or loss and the phase difference between the two input signals can be derived according the following equations given in the AD8302 datasheet:

$$V_{MAG} = V_{SLP} \log \left(\frac{V_{INA}}{V_{INB}} \right)$$
$$V_{PHS} = V_\phi \log \left(\frac{\phi(V_{INA})}{\phi(V_{INB})} \right)$$

where V_{SLP} and V_ϕ are the gain and phase slope respectively.

According to the AD8302 datasheet, the ideal transfer characteristics of the circuit are shown in Figure 1.

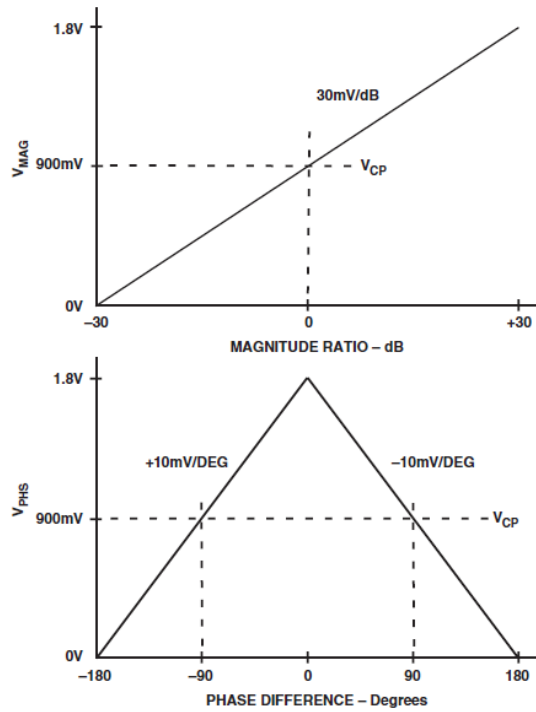


Figure 1: Nominal transfer functions.

3. Block diagram

Figure 2 shows the block diagram of the gain and phase detector with its auxiliary components for proper operation.

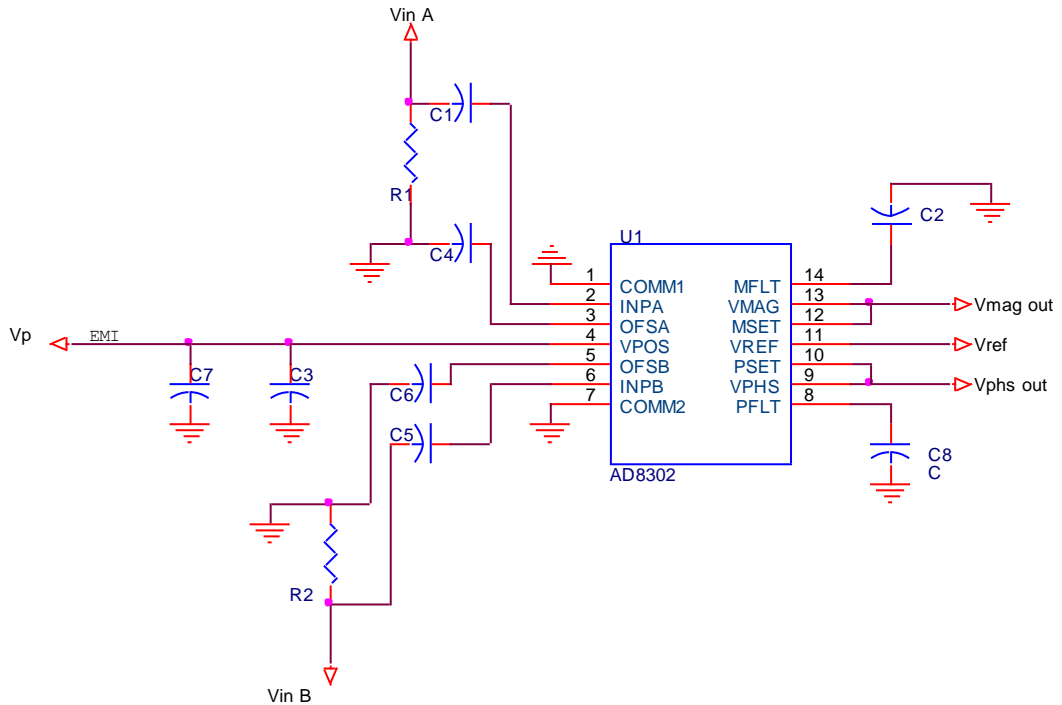


Figure 2: PCB schematic circuit.

The value of each component is shown in Table 1:

Component	Function	Value
R1, R2	Input Termination. Provide termination for input sources.	52.3Ω
C1, C5	Input AC-Coupling Capacitors.	1nF
C4, C6	Offset Feedback. These set the high-pass corner of the offset cancellation loop and thus with the input ac-coupling capacitors the minimum operating frequency.	1nF
C3	Supply decoupling.	1nF
C7	Supply decoupling.	50nF
EMI Filter	Filters the non desired frequency components of the DC supply signal.	NFE61P 4700 pF
C2, C8	These capacitors limit the video bandwidth of the gain and phase output respectively.	10nF

Table 1: PCB component's value.

4. PCB circuit design

The PCB circuit design has been performed with Cadstar 7.0 and translated to the LPKF milling machine code with CircuitCAM 4.0. The board layout can be seen in Figure 3. The board has been manufactured in CAY's electronic laboratory and the PCB vias has been metalized in the CAY's chemical lab.

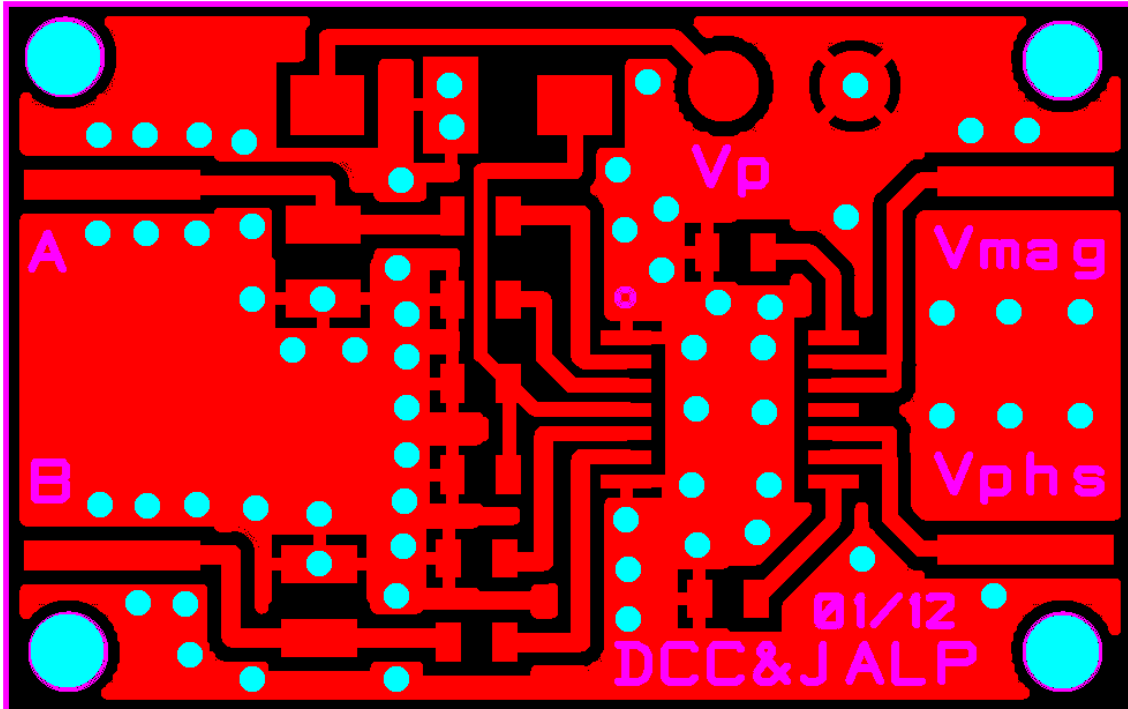


Figure 3: PCB layout view.

Figure 4 shows the final look of the PCB circuit outside the aluminum box and without interface connectors.

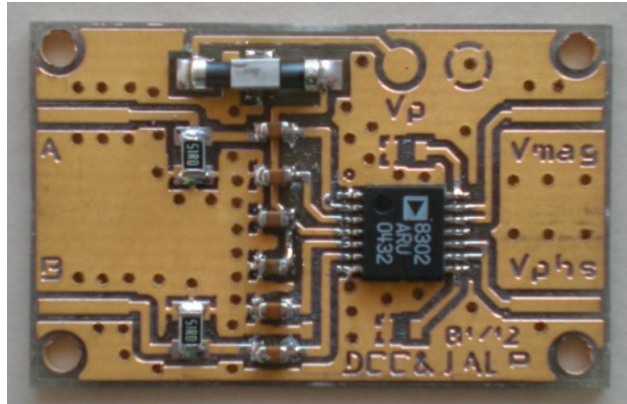


Figure 4: PCB circuit.

5. Measurements

The circuit is going to be evaluated at 10 MHz, 70 MHz (1st IF of holography receiver) and 150 MHz.

Two signal generators have been connected to A and B inputs of the gain & phase detector, and the voltage on Vmag and Vphs outputs are measured with a Tektronix digital oscilloscope. For phase measurements another digital oscilloscope has been used at the input of the system to control the phase difference between the signals in A and B. The cables from the signal generator to the gain & phase detector inputs have the same length. Similarly, the cables joining the signal generators and the Lecroy digital oscilloscope have equal length too.

Both signal generators are locked to the same external 10MHz reference signal, provided by one of them through a rear connector. The phase difference is controlled through a knob with the help of the phase function provided by the SMA 100A generator.

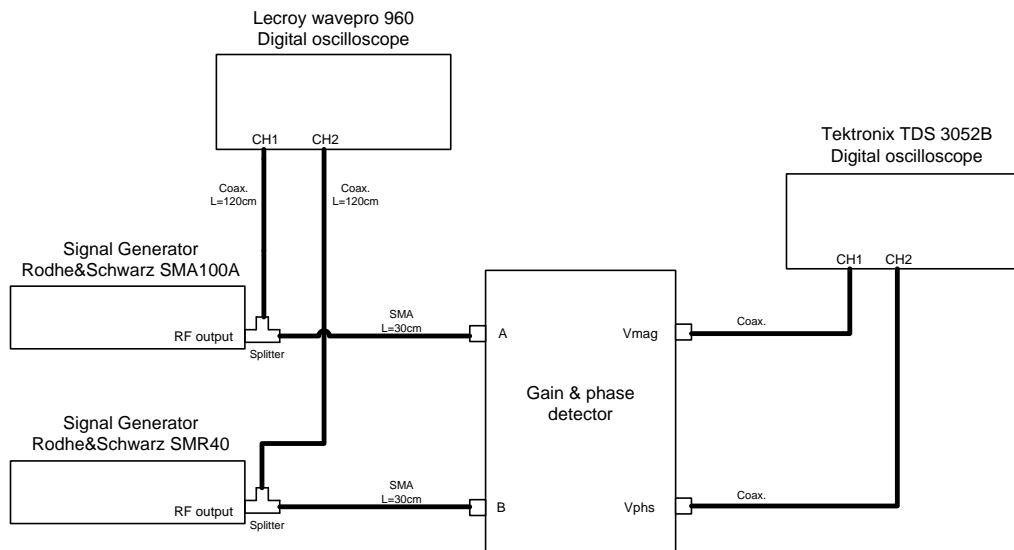


Figure 5: Gain and Phase Detector Test Bench.

The following tables and graphs show the measurements carried out according to the test bench shown in figure 5.

Frequency: 10 MHz				
V _{PHS}			V _{MAG}	
Ø _A -Ø _B (°)	V _{RMS} (V)	Scope Resolution	A (dBm)	B (dBm)
-180	0,027	20mV/div		-60
-165	0,109	0,5V/div		-55
-150	0,268	0,5V/div		-50
-135	0,435	0,5V/div		-45
-120	0,597	0,5V/div		-40
-105	0,757	0,5V/div		-35
-90	0,919	0,5V/div		-30
-75	1,08	0,5V/div		-25
-60	1,24	0,5V/div		-20
-45	1,4	0,5V/div		-15
-30	1,56	0,5V/div		-10
-15	1,72	0,5V/div		-5
0	1,79	1V/div		0
15	1,71	0,5V/div		
30	1,55	0,5V/div		
45	1,4	0,5V/div		
60	1,24	0,5V/div		
75	1,07	0,5V/div		
90	0,911	0,5V/div		
105	0,75	0,5V/div		
120	0,587	0,5V/div		
135	0,424	0,5V/div		
150	0,264	0,5V/div		
165	0,103	0,5V/div		
180	0,07	20mV/div		
			A (dBm)	B (dBm)
			Gain	V _{RMS} (V)
			Scope Resolution	
				-30
				-60
				-55
				-50
				-45
				-40
				-35
				-30
				-25
				-20
				-15
				-10
				-5
				0

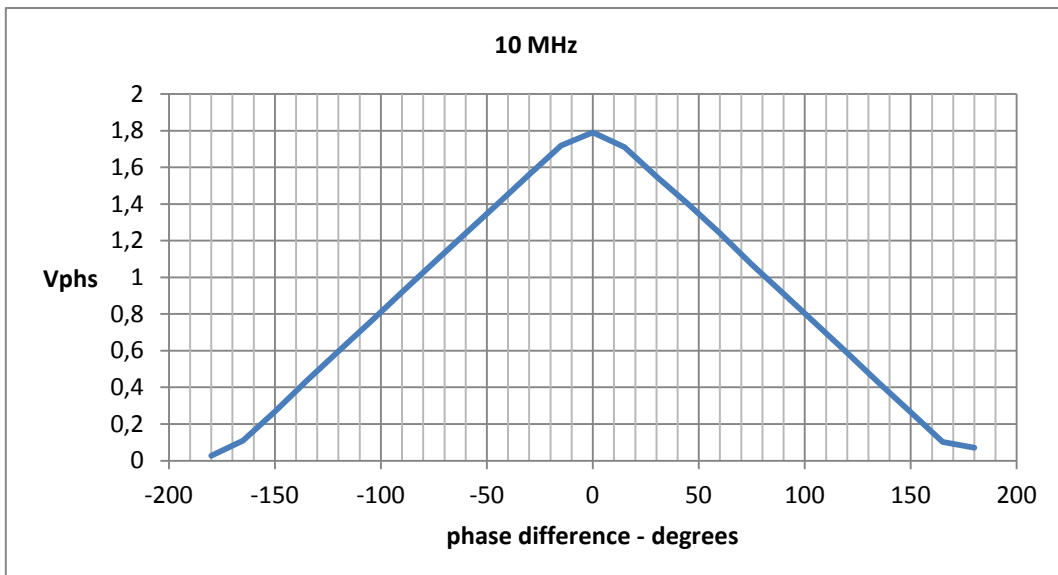


Figure 6: Measured phase difference at 10MHz.

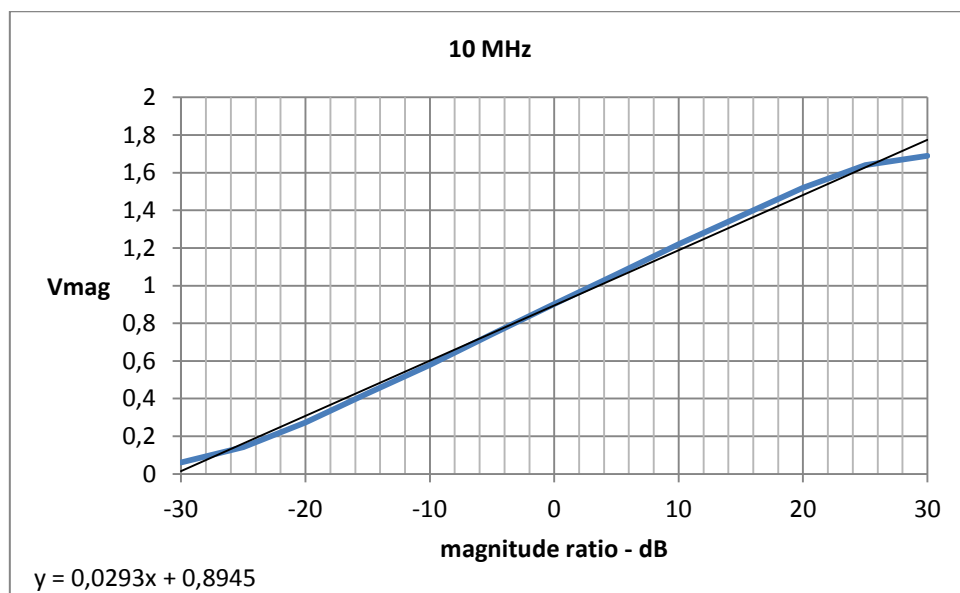


Figure 7: Measured gain at 10 MHz.

Frequency: 70 MHz				
V _{PHS}			V _{MAG}	
Ø _A -Ø _B (°)	V _{RMS} (V)	Scope Resolution	A (dBm)	B (dBm)
-180	0,027	20mV/div		-60
-165	0,132	0,5V/div		-55
-150	0,295	0,5V/div		-50
-135	0,429	0,5V/div		-45
-120	0,593	0,5V/div		-40
-105	0,756	0,5V/div		-35
-90	0,916	0,5V/div		-30
-75	1,08	0,5V/div		-25
-60	1,24	0,5V/div		-20
-45	1,4	0,5V/div		-15
-30	1,56	0,5V/div		-10
-15	1,72	0,5V/div		-5
0	1,78	1V/div		0
15	1,72	0,5V/div		
30	1,56	0,5V/div		
45	1,4	0,5V/div		
60	1,24	0,5V/div		
75	1,08	0,5V/div		
90	0,917	0,5V/div		
105	0,756	0,5V/div		
120	0,59	0,5V/div		
135	0,431	0,5V/div		
150	0,267	0,5V/div		
165	0,107	0,5V/div		
180	0,027	20mV/div		
			-30	-30

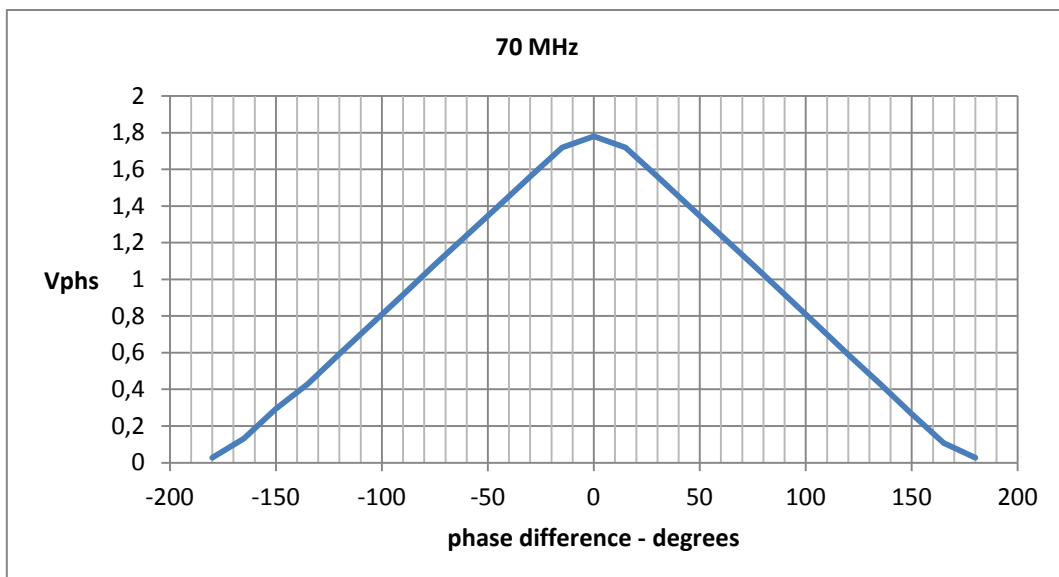


Figure 8: Measured phase difference at 70 MHz.

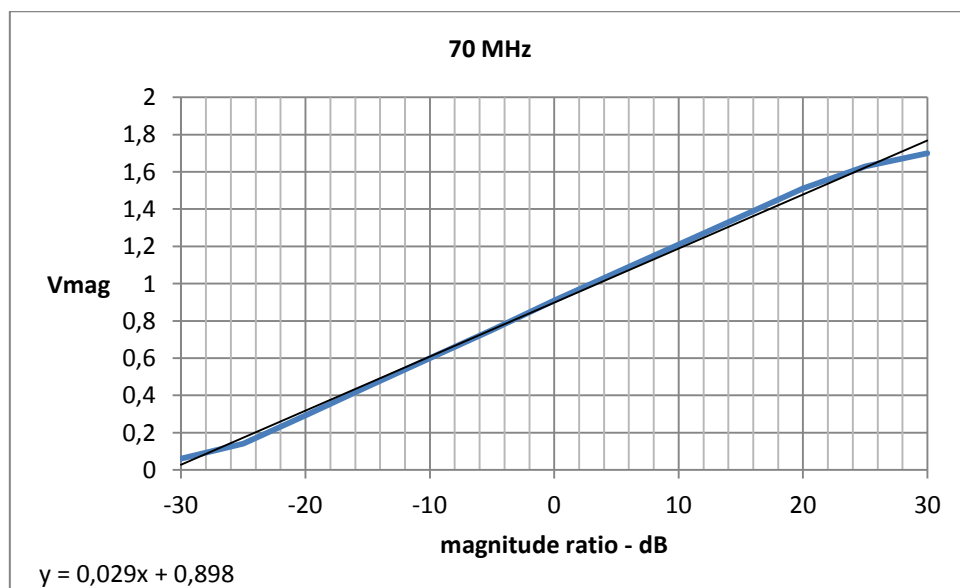


Figure 9: Measured gain at 70 MHz.

Frequency: 150 MHz							
Salida V _{PHS}			Salida V _{MAG}				
Ø _A -Ø _B (°)	V _{RMS} (V)	Scope Resolution	A (dBm)	B (dBm)			
-180	0,027	20mV/div		-60	30	1,7	500mV/div
-165	0,095	0,5V/div		-55	25	1,63	500mV/div
-150	0,252	0,5V/div		-50	20	1,51	500mV/div
-135	0,414	0,5V/div		-45	15	1,37	500mV/div
-120	0,58	0,5V/div		-40	10	1,22	500mV/div
-105	0,74	0,5V/div		-35	5	1,06	500mV/div
-90	0,902	0,5V/div		-30	0	0,915	500mV/div
-75	1,06	0,5V/div		-25	-5	0,76	500mV/div
-60	1,22	0,5V/div		-20	-10	0,6	200mV/div
-45	1,38	0,5V/div		-15	-15	0,45	200mV/div
-30	1,57	0,5V/div		-10	-20	0,296	200mV/div
-15	1,7	0,5V/div		-5	-25	0,146	200mV/div
0	1,78	1V/div		0	-30	0,062	20mV/div
15	1,73	0,5V/div					
30	1,56	0,5V/div					
45	1,41	0,5V/div					
60	1,25	0,5V/div					
75	1,09	0,5V/div					
90	0,927	0,5V/div					
105	0,764	0,5V/div					
120	0,604	0,5V/div					
135	0,442	0,5V/div					
150	0,282	0,5V/div					
165	0,12	0,5V/div					
180	0,027	20mV/div					

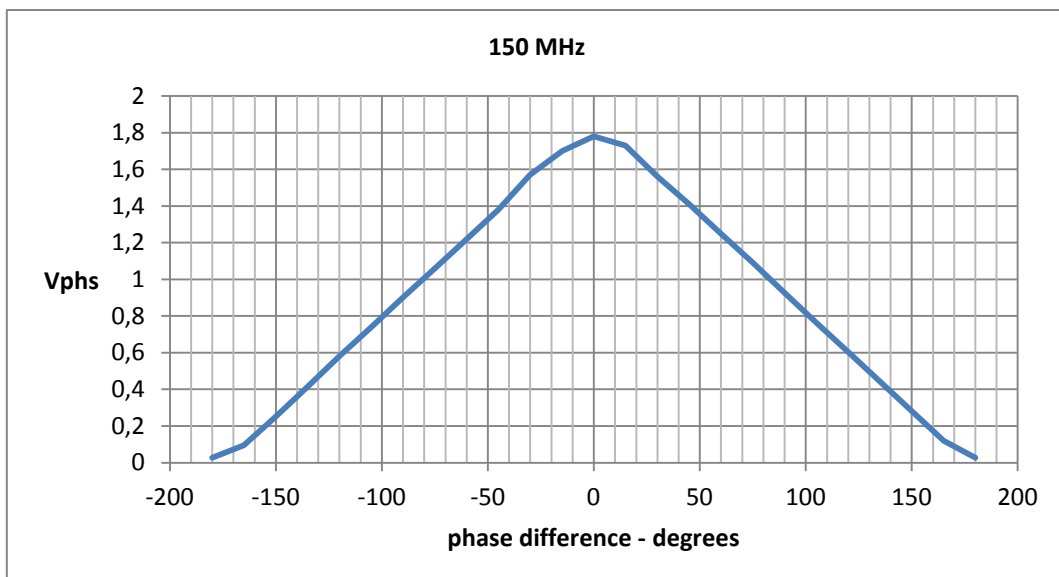


Figure 10: Measured phase difference at 150 MHz.

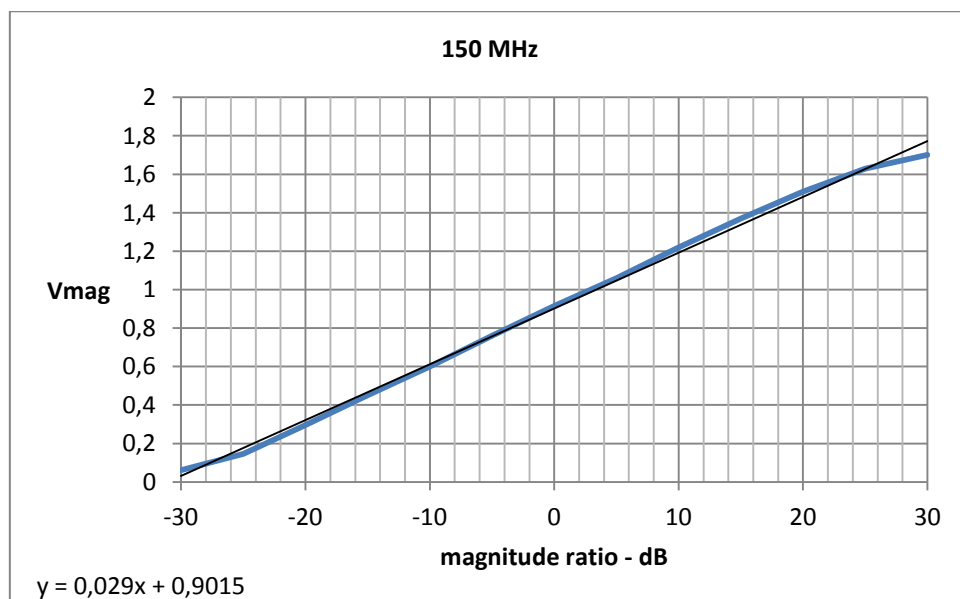


Figure 11: Measured gain at 150 MHz.

6. Conclusions

A prototype demonstration board for the AD8302 gain and phase has been designed to evaluate its capabilities. It operates from LF to 2.7GHz and it can detect gain differences from -30 dB to 30 dB and phase differences from -180° to +180°, according to its datasheet.

The circuit works according to the specifications at the measured frequencies. The results are summarized in the following table.

Frequency (MHz)	Vmag slope (mV/dB) Nominal value: 30mV/dB	Vphs slope (mV/°) Nominal value: 10 mV/°
10 MHz	29.3	±10.4
70 MHz	29.0	±10.3
100 MHz	29.0	±10.4

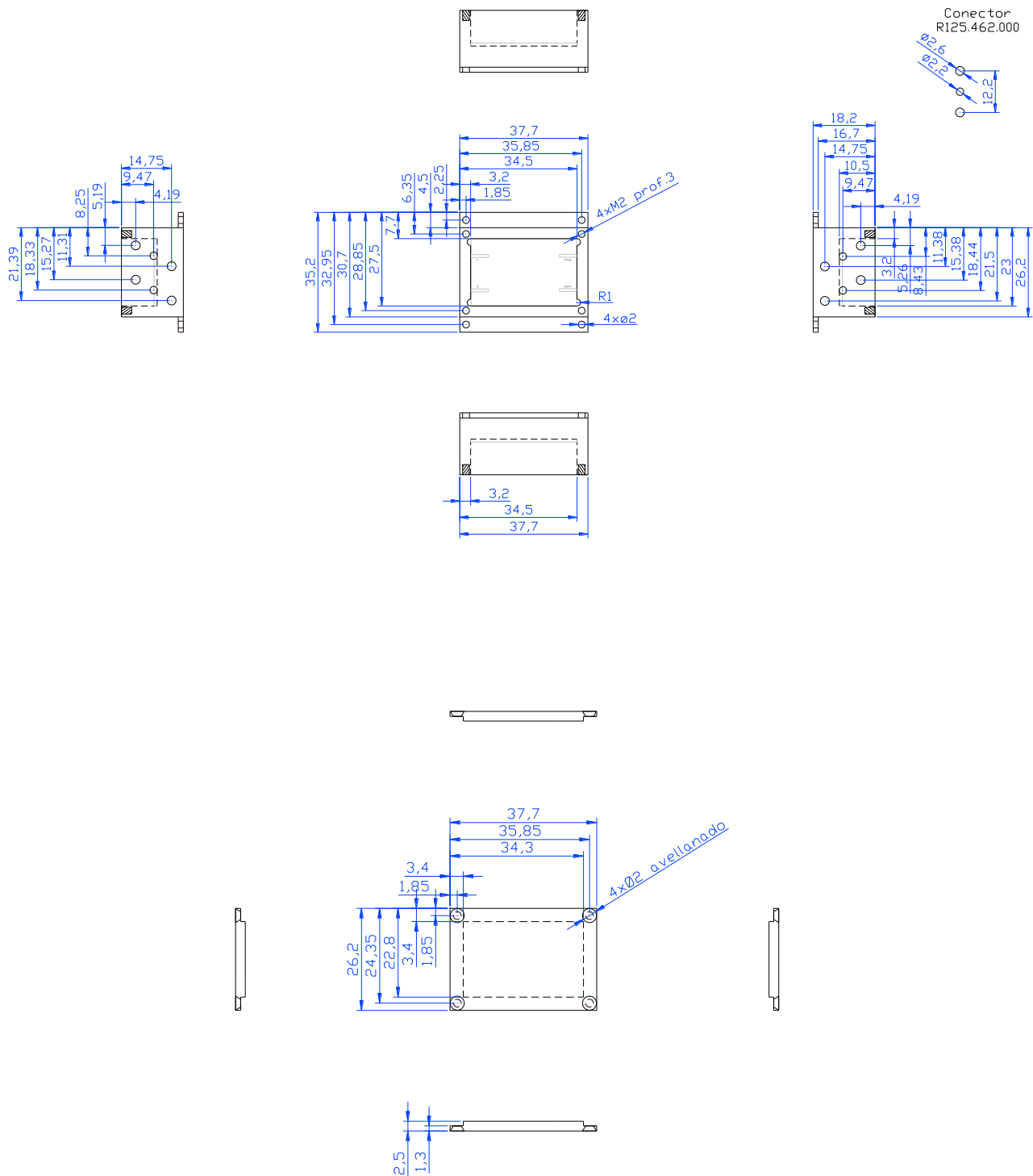
However, the phase response (Vphs) shows an ambiguity for the determination of the phase sign. For instance, at 150 MHz, if 1 V is measured at Vphs connector (figure 10), it is not possible to know whether the relative phase is +80° or -80°.

For this reason, this circuit could not be used for holography measurements, for example, unless than an additional circuit resolve the ambiguity could be envisaged.

7. Acknowledgments

The authors wish to thank the help provided by Carlos Almendros and Sergio Henche for the assembly of the board, José Manuel Hernández for the metallization of the vias and chemical finishing of the board and José María Yagüe for the manufacturing of the box enclosure.

Appendix A: Box enclosure drawings



Appendix B: Datasheets

The AD8302's datasheet is available at the analog devices web page:

http://www.analog.com/static/imported-files/data_sheets/AD8302.pdf